The degree and nature of radiation damage in zircon observed by 29 Si nuclear magnetic resonance

I. Farnan and E. K. H. Salje

Citation: Journal of Applied Physics **89**, 2084 (2001); doi: 10.1063/1.1343523
View online: http://dx.doi.org/10.1063/1.1343523
View Table of Contents: http://scitation.aip.org/content/aip/journal/jap/89/4?ver=pdfcov
Published by the AIP Publishing

The degree and nature of radiation damage in zircon observed by ^{29}Si nuclear magnetic resonance

I. Farnan[a] and E. K. H. Salje
Department of Earth Sciences, University of Cambridge, Downing Street, Cambridge CB2 3EQ United Kingdom

(Received 2 August 2000; accepted for publication 30 November 2000)

A quantitative analysis of ^{29}Si nuclear magnetic resonance spectra of radiation damaged, natural zircons showed that the local structure in crystalline and amorphous regions depend explicitly on radiation dose. Nonpercolating amorphous islands of high density ''glass'' within the crystalline matrix show a low interconnectivity of SiO_4 tetrahedra. This structural state is quite different from that of the high dose, percolating regions of low density glass with more polymerised tetrahedra. A continuous nonlinear dose dependence between the high and low density glass states is reported. A continuous evolution of the local structure of the crystalline phase up to the percolation point is also reported. No phase separation into binary oxides was observed. The total number of permanently displaced atoms per α-recoil event is $\sim$3800 atoms for low radiation doses and decreases to $\sim$2000 atoms for 10×10^{18} α events/g. No indication of partitioning of paramagnetic impurities between crystalline and amorphous regions was found for these natural zircons. The amorphous fractions of the metamict zircons were determined as a function of their accumulated radiation dose. These values coincide closely with those recently determined by x-ray diffraction studies. They are much greater than previously assumed based on density measurements. The dose dependence is consistent with the concept of direct impact amorphization in the atomic cascade following an α-recoil event.
 [DOI: 10.1063/1.1343523]

INTRODUCTION

The structural state of radiation damaged zircon is often described implicitly within a mixing model of two phases, namely, of the ''crystalline phase'' and the ''amorphous phase,'' e.g.[1–3] This approach would then allow the determination of the energetics of the two phases in a rather straightforward manner. While this idea of two phase mixing has the advantage of great simplicity we will argue that it is false. Instead, the structural states of both the crystalline and amorphous regions in zircon depend explicitly on the radiation dose. In most simple terms, this result was expected from the following argument. Zircon with low radiation damage is below the point at which the damaged regions start to percolate.[4] The damaged regions are fully encapsulated by a crystalline matrix which prevents the amorphous regions from swelling.[5] This means that the ''glass'' state is that of a high pressure glass while the crystalline part shows weak swelling. In fact, the crystal structure of zircon (crystalline parts only) was shown to be significantly different from the structure of totally undamaged zircon.[6] It was also shown that the phonon spectra of crystalline zircon show a dramatic softening below the first percolation point.[7] At slightly higher doses, both the crystalline and amorphous parts percolate. In this regime, the lattice parameters of crystalline zircon do not depend significantly on the radiation dose. At higher doses the second percolation point is passed at which point the crystalline regions become fully encapsulated by the amorphous matrix. In this regime the dose dependence of the molar volume virtually disappears.[4]

It was shown before that the structural state of the crystalline regions in zircon is significantly different in the three percolation regimes.[6,8] Perhaps more surprisingly, it was also argued that the specific volume of the amorphous glass regions is dramatically different in these three regimes, starting from a high density glass for low doses to a strongly dose dependent glass at intermediate doses to dose-independent densities for high doses. It takes little intuition to speculate that the short range glass structures should also show equivalent changes. We show in this article that this is indeed the case. We also confirm that volume proportions between amorphous and crystalline parts are essentially the same as those found by x-ray diffraction while very different from those that would be derived from a two phase mixing model.[1,9]

EXPERIMENTAL DETAILS

Zircon samples were obtained from a variety of sources but most were of Sri Lankan origin. All the samples except UG9A (powder) were single monolithic pieces of zircon ranging from 82 mg to over 400 mg in mass. The ages and uranium/thorium/lead isotopic ratios, where known, were used to calibrate their accumulated radiation doses, the remaining samples were calibrated using Raman spectroscopy.[7] All samples have been used in previous zircon studies (see Ref. 7 for summary). ^{29}Si nuclear magnetic resonance (NMR) experiments were carried out under magic

[a]Electronic mail: ifarnan@esc.cam.ac.uk

angle spinning (MAS). To do this a technique was developed where the rather large, for MAS, and irregularly shaped samples were packed in a slurry of $Pb(NO_3)_2$, with a density of 4.5 g cm^{-3}, which is intermediate between the densities of undamaged (4.7 g cm^{-3}) and fully metamict zircon (3.96 g cm^{-3}). This provided a more or less uniform mass distribution in the rotor and allowed the samples to be spun easily to speeds of over 5 KHz in a 7.5 mm diameter Chemagnetics MAS rotor.

The ^{29}Si NMR spectra were obtained on a Chemagnetics CMX400 and a Varian-Chemagnetics Infinity 400 spectrometer (9.4 T) both operating at 79.459 MHz and referenced to external tetramethylsilane (TMS). Typically several hundred FIDs were acquired from $\pi/10$ pulses (1 μs) with relaxation delays of several hundred seconds. In order to check for possible signal loss due to the presence of paramagnetic species in the samples, each sample was weighed and its signal intensity was compared with a standard. The fully relaxed spectrum of a weighed amount of potassium tetrasilicate glass was obtained under identical probe tuning and spectrometer conditions on a per scan per atom basis. This was then compared with the expected signal from each zircon sample to obtain the detection rate. Attempts were made to measure the spin-lattice relaxation times of certain samples (UG9A, Z5, Cam25). These showed a nonexponential recovery of relaxation and in most cases a signal intensity with a $\sqrt{t}$ dependence which is expected for relaxation by paramagnetic centres when there is no spin-diffusion.[10] Acquisition of the T_1 data was extremely time consuming (>2 days) and often full equilibrium was not reached. The relaxation delays used were optimized for spin-lattice relaxation times of 10 000 s which were consistent with the recovery rates observed. The integrated intensities of spectra acquired with shorter delays clearly showed that a large fraction of the signal was not being observed. The absolute intensity information allowed us to evaluate the efficacy of the delays used. The ^{29}Si detection rates obtained in this work ranged from 77% to 100% with an average of 88.1%. Some of this signal intensity is very likely not observed because of the adjacency of Si atoms to paramagnetic impurities and the remainder to sites with very long relaxation times.

RESULTS

Crystalline, undamaged, zircon shows a single sharp ^{29}Si NMR resonance at a chemical shift of -81.5 ppm.[11] This is characteristic of isolated SiO_4 tetrahedra or Q^0 in the Q^n notation, where n is the number of bridging oxygens bonded to quaternary (Q) silicon.[12] The ^{29}Si NMR spectrum of a zircon with a low number of accumulated α decays (Moroto, 1.0×10^{18} α/g) is compared with a more damaged heavily damaged one (Z5, 4.2×10^{18} α/g) in Fig. 1. The Moroto zircon has a chemical shift of -81.6 ppm and a line width of 65 Hz full width at half maximum. The difference between the two is the appearance in the spectrum of the more heavily damaged sample of a broad peak to low frequency of the crystalline peak with a center of gravity at -93.1 ppm and a width of ~1500 Hz and also a shifting and broadening of the crystalline peak to -83.7 ppm with a width of 340 Hz. This broad peak to low frequency of the crystalline zircon peak is assigned to amorphized regions in the damaged zircon. The series of spectra shown in Fig. 2 illustrate the increasing amount of damaged material that is detected in samples with a higher cumulative α-decay dose. The zircon with the highest dose (Sand4, 15.9×10^{18} α/g) shows only a single resonance for the amorphized material. Table I shows the relative amounts of crystalline and amorphous material detected for each sample. The relative proportions were determined at lower doses by least squares fitting of the spectra using a Lorentzian line shape for the crystalline contribution and an 80% Gaussian/20% Lorentzian for the amorphous contribution. This produced a good fit to the crystalline contribution but the broad, asymmetric amorphous peak was not well described by the single line shape. The amorphous fraction was

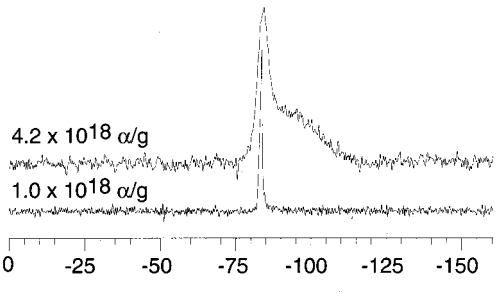

FIG. 1. ^{29}Si MASNMR spectra of zircons Z5 (upper) and Moroto (lower). Spectra were acquired with a spectral width of 20 kHz using $\pi/10$ pulses (1 μs) 182 pulses with a recycle delay of 180 s (Z5) and 265 pulses with a recycle delay of 270 s (Moroto). Samples were spun at 5.1 kHz and referenced to external TMS.

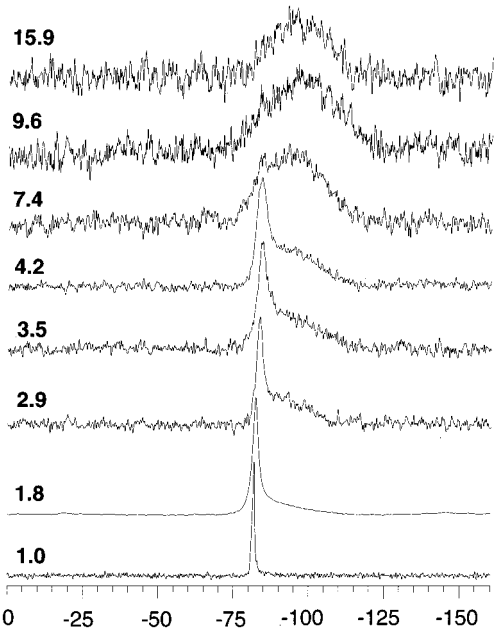

FIG. 2. Series of ^{29}Si MASNMR spectra of zircons with increasing accumulated α dose (upwards). Increasing numbers indicate the dose$\times10^{18}$ α events/g and refer to: Moroto, UG9A, Cam26, Cam25, Z5, Sand9, Ti8, and Sand4, respectively. Spectra were acquired as described in the text and referenced to external TMS.

TABLE I. Description of zircon samples used in this study.

Zircon	Origin	Mass (mg)	UO_2 content (wt %)	α dose ($\times 10^{18}\alpha$/g)	Amorphous fraction	Detection rate ^{29}Si (%)
Moroto	Uganda	126	0.02	1.0	<0.05[a]	84.4
UG9A	Uganda	534	0.10	1.8	0.33	77.0
Cam26	Sri Lanka	152	0.16	2.9	0.47	104.4[b]
Cam25	Sri Lanka	117	0.31	3.5	0.57	103.4[b]
z5	Sri Lanka	448	0.29	4.2	0.57	92.6
Sand9	Sri Lanka	149	0.49	7.4	0.95	84.7
Ti8	Sri Lanka	128	0.55	9.6	0.97	83.0
Sand4	Sri Lanka	82	1.02	15.9	1.0	83.1

[a]Maximum that could be present by considering detectability of the broad amorphous peak in the spectrum.
[b]Error is $\pm 5\%$ on ^{29}Si detection rate.

finally determined by subtracting the fitted crystalline contribution from the total integral for the signal (from -70 to -120 ppm). A similar procedure was used for doses above $2.9\times 10^{18}\,\alpha$/g except that the crystalline peak was fitted with a Gaussian line shape. Changing the initial conditions of the fits and the Lorentzian/Gaussian ratio of the line shape used to describe the amorphous peak produced variations of 1%–3% in the relative areas of the peaks. The final column of Table I shows the detection rate for ^{29}Si in each sample. This was obtained by comparing the total signal intensity for each zircon (per scan, per atom) with the signal from a fully relaxed spectrum, taken under similar conditions of probe tuning, of a known mass of potassium tetrasilicate glass. The errors in integrating spectra with broad lines and relatively high noise appear to be $\pm 5\%$.

The chemical shifts of both the crystalline and amorphous peaks appear to evolve systematically with increasing α dose, this is shown in Fig. 3. The shift of the crystalline peak shows a break in slope at a dose of $3.5\times 10^{18}\,\alpha$/g(Cam25) and the peak remains constant at -84 ± 0.3 ppm for higher α doses. A similar break in slope occurs for the center of gravity of the amorphous peak at a dose of $4.2\times 10^{18}\,\alpha$/g. The evolution of the resonance of the amorphous phase with increasing dose can be seen in Fig. 4 where the spectra of four zircons have been plotted together with the spectrum of the most heavily damaged sample, Sand4. The amorphous line shapes of the two most heavily damaged samples, Ti8 and Sand4 [Fig. 4(a)], appear to be the same within the signal to noise of the spectra, whereas the amorphous line shape of Sand9 [Fig. 4(b)] shows some excess intensity to high frequency of Sand4. The samples Cam26 [Fig. 4(c)] and UG9A [Fig. 4(d)] show greater deviations in the position and shape of the amorphous peak. Each indicate that the higher the α dose the greater the intensity at low frequency, more negative chemical shifts. The amorphous line shape of UG9A is ''concave,'' like a tail to the crystalline peak, rather than rounded like the higher dose samples.

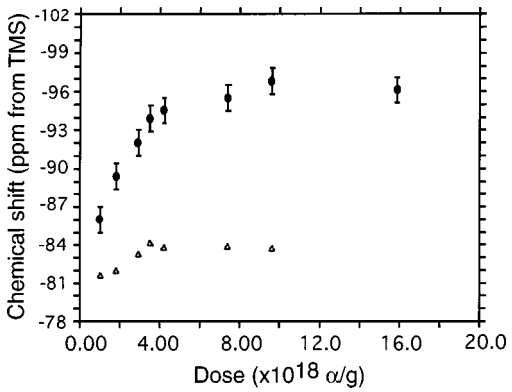

FIG. 3. Chemical shift of the amorphous (closed circles) and crystalline (open triangles) phases as a function of accumulated α dose. The crystalline peak position is derived from the fitting process, the amorphous peak position represents the center of gravity of the remaining intensity once the crystalline peak has been subtracted.

DISCUSSION

The ^{29}Si MASNMR spectra presented here show that good quality ^{29}Si spectra can be obtained from zircons across the range of α-decay damage from almost perfectly crystalline to completely amorphous. In each case we have verified that the observed NMR signal was at least 77%, and in some cases 100%, of the silicon atoms in the sample by comparing signal intensities with a standard. We note that very rarely in the literature are absolute silicon NMR intensities checked against a standard in this way and these rates of detection may well be standard. We also have fairly good evidence that the relative intensities that we observe in our spectra are representative of the total amounts of amorphous and crystalline regions in the zircons. Very long silicon spin-lattice relaxation times were observed for all the samples and only minor changes in relative intensities accompanied the large changes in absolute intensity observed for increased relaxation delays from 1 to 3000 s following a saturation comb of 16 90° pulses. This effect is shown for zircon Z5 in Fig. 5. This indicates that paramagnetic species responsible for relaxation are fairly evenly distributed between amorphous and crystalline regions. It is an additional concern that when paramagnetic species are present in samples used for NMR experiments that not only is some signal lost but the resonances may be shifted paramagnetically and/or lifetime broadened by rapid relaxation. In this scenario, linewidths which would normally be attributed to a distribution of sites may in fact be a single broad line. Although we have long T_1's in these samples we did check that the broad lines we

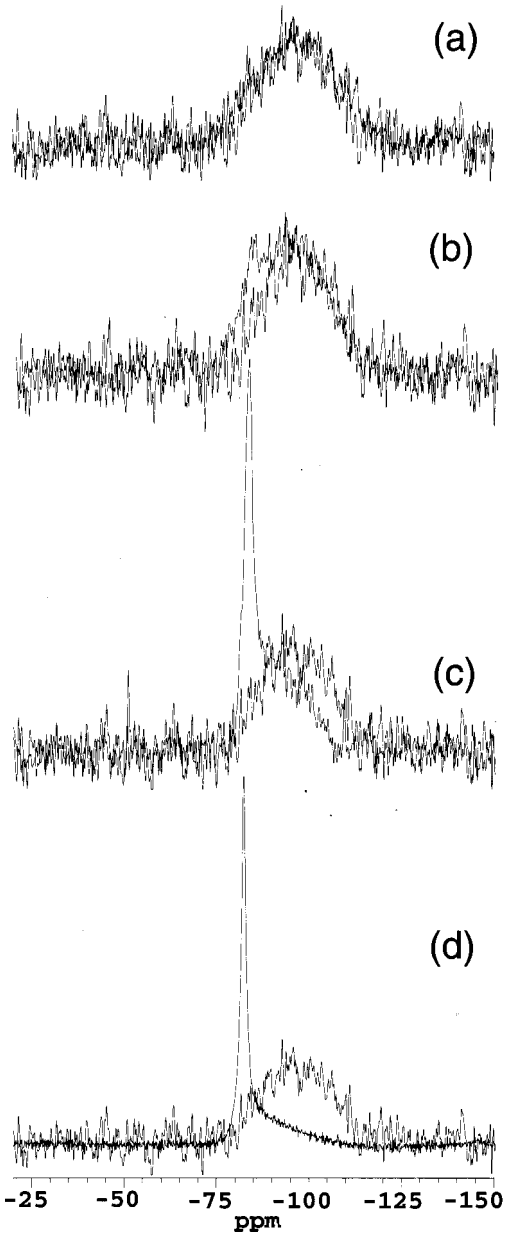

FIG. 4. A comparison of the most heavily damaged sample, Sand4 (15.9×10^{18} α decays/g), completely amorphous with the amorphous regions of various zircons containing crystalline and amorphous regions. (a) Sand4 vs Ti8 (9.6×10^{18} α/g). (b) Sand 4 vs Sand9 (7.4×10^{18} α/g), (c) Sand 4 vs Cam26 (2.9×10^{18} α/g), and (d) Sand 4 vs UG9A (1.8×10^{18} α/g).

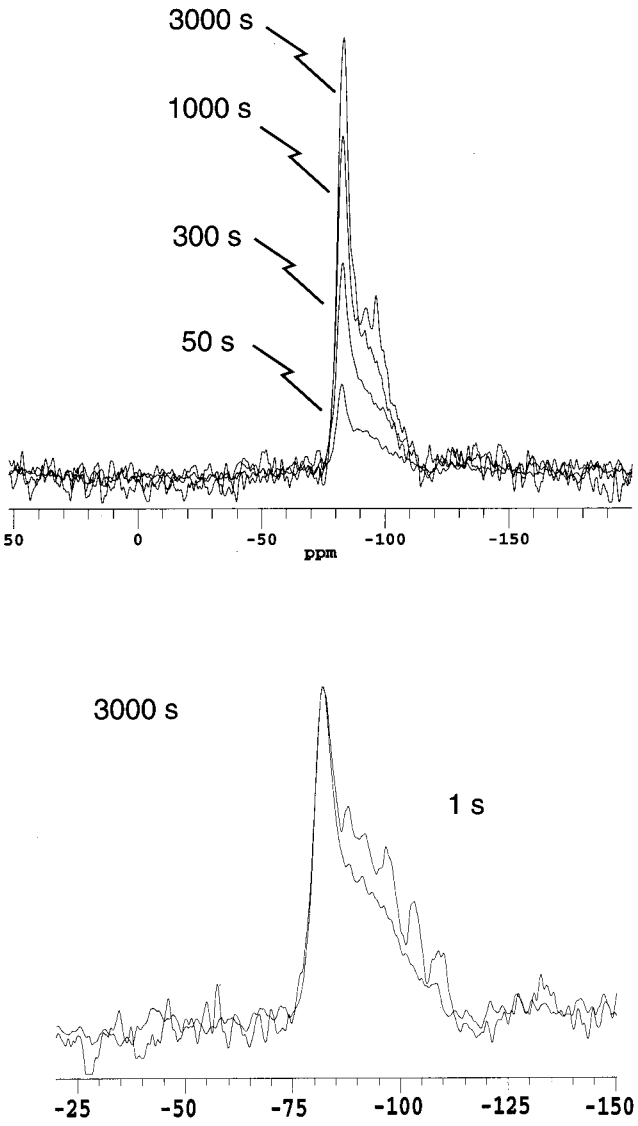

FIG. 5. Upper: Increase in ^{29}Si signal intensity as a function of relaxation delay following a saturation comb of 16 rf pulses. Lower: comparison of the ^{29}Si MASNMR spectra acquired with different relaxation delays, note the small difference in going from 1 to 3000 s in the relative abundance of each phase.

observe are due to distributions of sites. Using a ''Hahn echo'' we monitored the intrinsic NMR linewidth by applying echo delays out to 8 ms. Figure 6(a) shows that echo intensity has diminished very little after 8 ms and implies that we have a very narrow intrinsic line width ($<$40 Hz) with distributions of chemical shifts as the origin of the line widths in these samples. Figure 6(b) shows the Fourier transform of the echo after 8 ms compared with the single pulse spectrum of Z5 and there is virtually no difference. We also note that the shifts observed in the spectra in going from undamaged zircon to fully metamict zircon are all diamagnetic and thus can reasonably be interpreted as changes in ^{29}Si chemical shifts and thus real changes in Si local environments rather than due to interactions with unpaired electrons.

The fraction of silicon atoms detected in the amorphous phase of zircon is plotted against the cumulative α dose in Fig. 7. This data is compared with the data of Rios *et al.*,[6] open circles, and the double overlap model discussed by Weber *et al.*[1] The error bars in the fraction of Si in the amorphous phase are determined from the uncertainty in the observed silicon NMR signal. Where detection rates were 100% the error bars were determined from the errors in the fitting and were less than the size of the symbols in some cases. The degree of damage as a function of cumulative α dose detected by ^{29}Si NMR is clearly greater than the derived values of amorphous volume fraction previously estimated by Weber *et al.* and fitted to the double overlap model. The data are in good agreement with the data of Rios *et al.* who

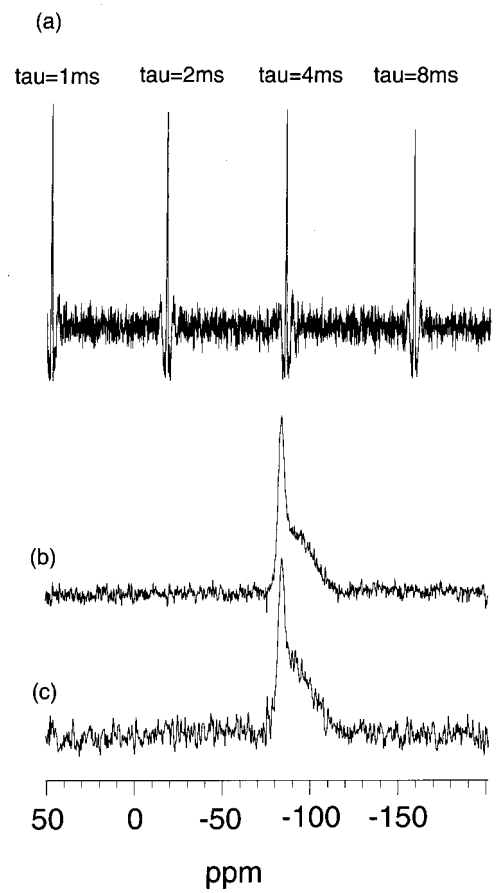

FIG. 6. (a) Time domain signals following a 90°-τ-180°-acquire Hahn echo pulse sequence with tau delays as indicated applied to zircon Z5. Echo intensity diminishes slightly at $\tau = 8$ ms indicating a very narrow intrinsic line width (long T_2) for the ^{29}Si resonances observed, i.e., linewidth is determined by an inhomogeneous distribution of chemical shifts, (b) spectrum obtained by Fourier transform of the single pulse free induction decay of Z5, and (c) spectrum obtained by Fourier transform taken from the peak of the 8 ms echo in (a).

determined the x-ray scattering intensity of the amorphous fraction as a function of α dose. They concluded that the amorphous fraction could be fairly well explained by direct amorphization occurring in the cascade of atoms produced by the recoil of the α-emitting nucleus. The fraction of Si atoms in the amorphous phase can be used to estimate the total number of atoms permanently displaced in the α-recoil cascade. The number of α decays per mole is equated with the number of atoms displaced per mole to obtain the number of Si atoms permanently displaced, this is multiplied by the number of atoms in the Zircon formula unit (6) to obtain the total number of atoms displaced. Figure 8 shows that 3615 atoms were permanently displaced per α decay in UG9A and this decreases to 1995 atoms for Ti8. Presumably, this decrease with cumulative dose is due to overlap of some kind, i.e., areas being hit more than once and so contributing fewer atoms to the total number of atoms permanently displaced. A linear extrapolation to zero dose gives 3782 atoms displaced per α decay. This corresponds to a radius of 21.4 Å for a damaged region, or ''amorphous core,'' resulting from a single α-recoil event (cascade formation and subsequent relaxation). This is in reasonable agreement with the 50 Å

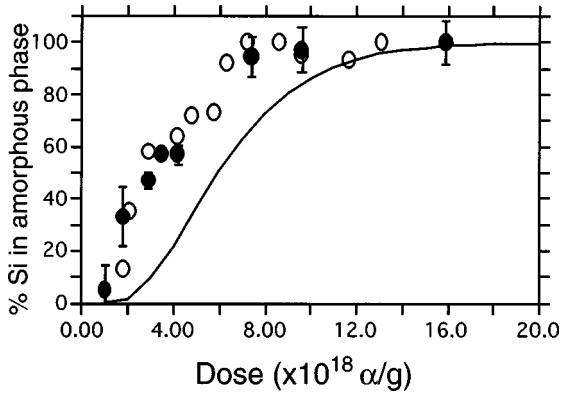

FIG. 7. The fraction of Si in the amorphous phase of the zircons studied plotted as a function of accumulated α dose (closed circles). Also plotted are the x-ray diffraction data of Rios *et al.* for the amorphous fraction (open circles) and the double overlap model used by Weber *et al.* to fit the previous amorphous fractions determined from density measurements (solid line).

diameters of damaged regions observed by transmission electron microscopy (TEM) in low dose samples.[13]

The ^{29}Si NMR spectra distinguish clearly between the crystalline and amorphous regions of the damaged zircons. It is also clear from Fig. 3 that the chemical shift changes observed as a function of cumulative α dose indicate an evolving local structure in both the crystalline and the amorphous regions. As a consequence any interpretation of radiation damage as a two phase process including an amorphous phase and a crystalline phase is not correct. For example, the center of gravity of the broad amorphous peak increases from -89.5 ppm in UG9A(1.8×10^{18} α/g) to -96.1 ppm for Sand4(15.9×10^{18} α/g). This evolution of the local structure of the amorphous phase with dose appears to be saturated at an α dose slightly above 4.2×10^{18} α/g. The evolution of the changes in the crystalline peak position also saturate at a slightly lower dose (3.5×10^{18} α/g). This dose is consistent with diffuse scattering data[4] where the spontaneous strain in the crystalline fraction goes to zero as the amorphized re-

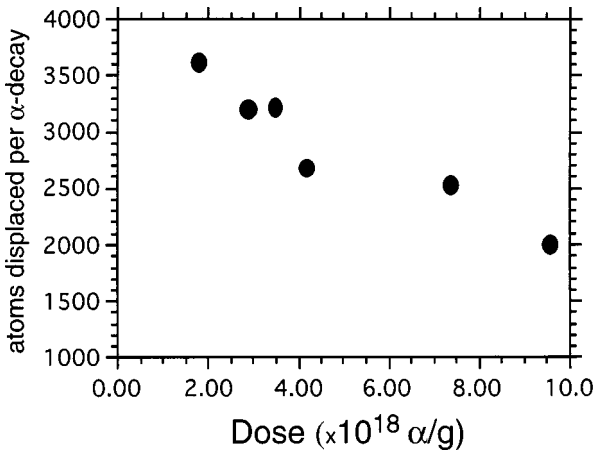

FIG. 8. Plot of the number of atoms permanently displaced per α-decay event as a function of accumulated α dose. The total number of atoms permanently displaced is calculated from the fraction of Si atoms permanently displaced on the basis of the zircon formula unit ($ZrSiO_4$), i.e., six times N(Si).

gions in zircon form a percolating cluster. A second percolation point, suggested in the diffuse x-ray scattering work, occurs where the macroscopic volume no longer changes, i.e., between $4.2\times10^{18}\,\alpha$/g(z5) and $7.4\times10^{18}\,\alpha$/g(Sand9). This is consistent with the saturation of changes in the local structure of the amorphous phase observed by ^{29}Si NMR. The amorphization process at low α dose consists of amorphous islands constrained within a crystalline matrix. This then inverts to a system of crystalline islands within an amorphous matrix at higher doses. At lower doses the amount of amorphous material detected by ^{29}Si NMR is significantly higher than predicted from macroscopic volume measurements, i.e., there is a lot of amorphous phase with little swelling. This can only be accommodated if the amorphized phase is effectively under a confining pressure exerted by the crystalline matrix. An interpretation of the local structural changes that are occurring in the amorphous phase of zircon can be made based on the large body of data obtained from ^{29}SiNMR spectra of silicates.[12,14] The ^{29}Si chemical shift for silicon in fourfold coordination with oxygen depends on the nature of the Si second neighbor. The clearest and largest effect is whether this second neighbor is another Si atom, i.e., whether the oxygen is bridging or nonbridging. First of all, an empirical scale of chemical shifts based on the chemical shifts in alkali silicate glasses with varying degrees of polymerization[15] would indicate that the amorphous phase of zircon contains Si–O–Si linkages that do not exist in the undamaged crystalline phase. The exact extent of the average polymerization depends upon a nonunique interpretation of the structure–shift relationship. The amorphous phase in UG9A($1.8\times10^{18}\,\alpha$/g) has an average shift of -89.5 ppm. In alkali silicate glasses, for which there is the largest amount of data on amorphous silicates, this would fall clearly in the middle of the range indicative of two Si second neighbors (Q^2). On this scale, also, the average number of Si second neighbors in Sand4($15.9\times10^{18}\,\alpha$/g), chemical shift -96.1 ppm, is three (Q^3). However, the nature of the network modifying cation also has an effect on the chemical shift. Zirconium appears to cause the shift of the isolated Q^0 in zircon to be at the very end of the range for Q^0 species in crystalline phases that do not contain aluminum (from -60 to -81.6 ppm). This may mean that in the amorphous zircon phase the scale is shifted and a change in shift from -81.6 to -107.1 ppm (quartz) would be appropriate for the complete range of Si tetrahedral environments from Q^0 to Q^4. Within this interpretation, the average polymerizations would lie between Q^1 and Q^2 in UG9A and between Q^2 and Q^3 for Sand4. We note also that the shifts of Q species in alkali silicate glasses change with composition. For example a Q^3 site in $Na_2Si_4O_9$ glass occurs at -92.5 ppm whereas the same site in Na_2SiO_3 glass occurs at -84.8 ppm.[15] This might suggest that glasses with lower amounts of SiO_2 would show somewhat lower shifts for equivalent Q species than in more SiO_2 rich glasses. Whatever the subtleties of the structural interpretation, both of these peaks cover nearly the whole range of resonance positions observed in crystalline and glassy silicates for Si Q^n species[12] and average polymerization increases significantly with α dose. We note that all resonances for the amorphous contributions to

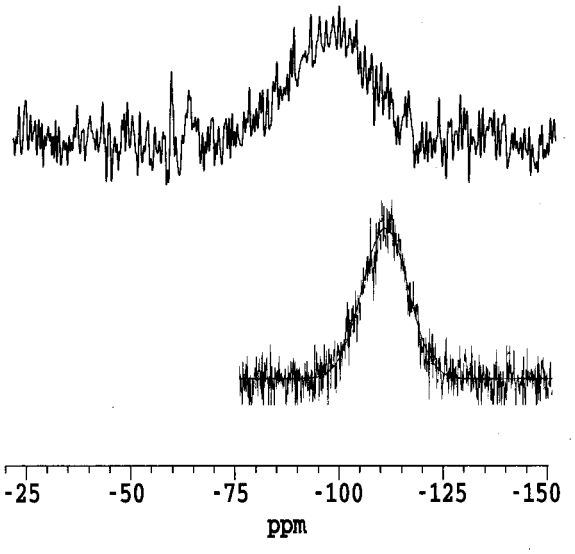

FIG. 9. Comparison between the ^{29}Si MASNMR spectrum of melt-formed SiO_2 glass and the most heavily damaged, and completely amorphous zircon Sand 4 ($15.9\times10^{18}\,\alpha$/g). The SiO_2 glass was made by melting cristobalite ($Si^{17}O_2$) at 1800 °C in a molybdenum capsule, the water and impurity contents are not known but are believed to be very low. Sand4 spectrum acquired with 783 π/10 pulses with a 100 s recycle delay and SiO_2 glass acquired with 180 π/12 pulses with 300 s delay.

the spectra fall to the baseline between -116 and -120 ppm. This is consistent with the known range of chemical shifts for Si in fourfold coordination with oxygen and Q^4 resonances in silicate glasses. We can compare the spectrum of Sand4 and a melt-formed SiO_2 glass in Fig. 9. There is a clear difference between the melt-formed glass and the fully metamict zircon and indeed an even greater difference between the amorphous peaks of lower damage zircons and the melt-formed SiO_2 peak. Although an amorphous SiO_2 phase is observed in annealed zircon samples,[16,17] there is little evidence of it originating in the initial in-cascade amorphization. It must be formed following thermally activated diffusion during annealing. The ^{29}Si MASNMR spectra indicate some ''fully polymerized'' Q^4 species (silicalike) but these are part of a very wide distribution of Q species in the amorphous zircon regions. A broad distribution of Q species is what might be expected for a glass quenched at a very high rate.[18] This may be the type of amorphization that occurs in zircon. Simulation studies of radiation damage in metals[19,20] show that following the ballistic recoil of the α-emitting nucleus there is a localized thermal spike in the cascade where energies exceed the heat of fusion. Similar effects are believed to occur in zircon[21] and recent molecular dynamics simulations on zircon itself show that this thermal spike is then quenched in only a few picoseconds.[22]

There are two implications of this direct amorphization mechanism which need to be accounted for. The first is the fate of oxygen atoms following the formation of the amorphous core of the cascade. The presence of bridging oxygens in a connected silicate network means that fewer oxygens are (structurally) required in the structure of the combined crystalline and amorphous phase than in the purely crystalline phase, although charge balance must still be obeyed. In un-

damaged zircon each Si has four oxygens associated with it in an isolated SiO_4 tetrahedron. In an amorphous phase with an average speciation of Q^2 then there are on average three oxygens per SiO_4 tetrahedron. This means for UG9A, for example, for each silicon atom in the amorphous phase there is one oxygen unaccounted for an in Sand4 or Ti8 there are ~1.5 oxygens unaccounted for per SiO_4 tetrahedron. Zr-edge extended x-ray absorption fine structure data on zircons with increasing cumulative α dose[23,24] show that the average oxygen coordination number of zirconium decreases from 8 to 7 in going from lightly damaged to fully metamict zircon. One interpretation is that the zirconium polyhedra have changed their connectivity and have gone from corner sharing to distorted edge sharing polyhedra similar to those in baddelyite (monoclinic ZrO_2). This would create Zr–O–Zr oxygens and thus allow a Si–O–Si bond to form. However, one Si–O–Si bridge per zirconium would only account for Q^1 average polymerization. A significant number of oxygens are probably lying in interstitial sites both in the amorphous phase and the crystalline phase. Recent *ab initio* electronic structure (total energy) calculations[25] of interstitial defects in zircons indicate that pairs of interstitial oxygens could form a ''dumbell'' type defect in the crystalline phase. Very recent molecular dynamics simulations of radiation damage in zircon[22] also indicate substantial numbers of interstitial oxygens in the damaged amorphous regions.

The evolution of the chemical shift of the crystalline phase from −81.6 to −84 ppm and its fivefold increase in width from 65 to 340 Hz would indicate significant disorder occurring within the crystalline structure. Obvious contributions to this would be recrystallized, defect rich areas surrounding the amorphous core of a cascade and undamaged but strained areas surrounding the damaged (crystalline and amorphous) regions. Both oxygen vacancies and interstitial oxygen defects would be present in the rapidly recrystallized regions arising from α recoil, but they may also occur due to direct flights (and stoppings) of α particles which are thought to cause ionizations and 100–200 displaced atoms in the crystalline material.[26] The increasing negative chemical shifts of the crystalline peak may be indicative of more polymerized Si environments in the crystalline phase as well as the amorphous phase. Si–Si distances are quite small (3.6 Å) in the alternating chains of isolated tetrahedra and the displacement of an oxygen and a slight rotation of the tetrahedra could result in the formation of a dimer or a short chain. Either of these situations would cause a more negative Si chemical shift. However, in general, this would be expected to be a somewhat larger shift than the 4–5 ppm which represents the low frequency side of the distorted crystalline zircon peak.

CONCLUSIONS

Radiation damage in zircon, as detected by the fraction of silicon atoms present in an amorphous phase, is found to be considerably higher than previously estimated. The degree of damage is essentially consistent with direct amorphization in the cascade following the recoil of an α-emitting nucleus. The local structure around Si in both the crystalline and amorphous regions evolves systematically with α dose. The average polymerization of the amorphous phase at low dose of approximately two bridging oxygens per SiO_4 tetrahedron increases to approximately three bridging oxygens per tetrahedron in a fully metamict zircon with no discrete amorphous SiO_2 phase being observed. Models of radiation damage in zircon which envisage the process as simply a change in the relative proportions of crystalline and amorphous phases as a function of α dose are not appropriate. A large number of interstitial defect oxygen sites need to be present in order to rationalize the polymerized structure of the amorphous phase. These might well be detected in future work by oxygen-17 NMR.

ACKNOWLEDGMENTS

The authors would like to thank M. Zhang for help with sample characterization, F. Farges and an anonymous reviewer for helpful comments, and finally the EPSRC (UK) for funding (JREI GR/M35406).

[1] W. J. Weber, R. C. Ewing, and L. M. Wang, J. Mater. Res. **9**, 688 (1994).
[2] R. C. Ewing, Nucl. Instrum. Methods Phys. Res. B **91**, 22–29 (1994).
[3] S. Ellsworth, A. Navrotsky, and R. C. Ewing, Phys. Chem. Miner. **21**, 140 (1994).
[4] E. K. H. Salje, J. Chrosch, and R. C. Ewing, Am. Mineral. **84**, 1107 (1999).
[5] K. Trachenko, M. T. Dove, and E. Salje, J. Appl. Phys. **87**, 7702 (2000).
[6] S. Rios, E. K. H. Salje, M. Zhang, and R. C. Ewing, J. Phys.: Condens. Matter **12**, 2401 (2000).
[7] M. Zhang, E. K. H. Salje, I. Farnan, A. Graeme-Barber, P. Daniel, R. C. Ewing, A. M. Clark, and H. Leroux, J. Phys.: Condens. Matter **12**, 1915 (2000).
[8] M. Zhang, E. K. H. Salje, G. C. Capitani, H. Leroux, A. M. Clark, J. Schluter, and R. C. Ewing, J. Phys.: Condens. Matter **12**, 3131 (2000).
[9] W. J. Weber, J. Am. Ceram. Soc. **76**, 1729–1738 (1993).
[10] F. Devreux, J.-P. Boilot, F. Chaput, and B. Sapoval, Phys. Rev. Lett. **65**, 614 (1990).
[11] M. Magi, E. Lippmaa, A. Samoson, G. Engelhardt, and A. R. Grimmer, J. Phys. Chem. **88**, 1518 (1984).
[12] G. Engelhardt and D. Michel, *High Resolution Solid State NMR of Silicates and Zeolites* (Wiley, New York, 1987).
[13] G. C. Capitani, H. Leroux, J. C. Doukhan, S. Rios, M. Zhang, and E. K. H. Salje, Phys. Chem. Miner. **27**, 545 (2000).
[14] J. F. Stebbins, in *Mineral Physics and Crystallography, A Handbook of Physical Constants*, edited by T. J. Ahrens (American Geophysical Union, Washington DC, 1995), pp. 303–331.
[15] H. Maekawa, K. Maekawa, K. Kawamura, and T. Yokokawa, J. Non-Cryst. Solids **127**, 53 (1991).
[16] A. C. McLaren, J. D. Fitzgerald, and I. S. Williams, Geochim. Cosmochim. Acta **58**, 993 (1994).
[17] M. Zhang, E. K. H. Salje, R. C. Ewing, I. Farnan, S. Rios, J. Schluter, and P. Leggo, J. Phys.: Condens. Matter **12**, 5189 (2000).
[18] J. F. Stebbins and I. Farnan, Science **245**, 257 (1989).
[19] D. J. Bacon and T. D. d. l. Rubia, J. Nucl. Mater. **216**, 275 (1994).
[20] H. L. Heinisch and B. N. Singh, Philos. Mag. **67**, 407 (1993).
[21] A. Meldrum, S. J. Zinkle, L. A. Boatner, and R. C. Ewing, **395**, 56 (1998).
[22] K. Trachenko, M. T. Dove, and E. K. H. Salje, Phys. Rev. Lett. (submitted).
[23] F. Farges and G. Calas, Am. Mineral. **76**, 60 (1991).
[24] F. Farges, Phys. Chem. Miner. **20**, 504 (1994).
[25] J. P. Crocombette, Phys. Chem. Miner. **27**, 138 (1999).
[26] W. J. Weber, **5**, 2687 (1990).